

Monte Carlo Simulation of the $SU(2)/\mathbb{Z}_2$ Yang–Mills Theory

Motokazu Abe¹, Okuto Morikawa², and Hiroshi Suzuki¹

¹*Department of Physics, Kyushu University, 744 Motoooka, Nishi-ku,
Fukuoka 819-0395, Japan*

²*Interdisciplinary Theoretical and Mathematical Sciences Program
(iTHEMS), RIKEN, Wako 351-0198, Japan*

.....
We carry out a hybrid Monte Carlo (HMC) simulation of the $SU(2)/\mathbb{Z}_2$ Yang–Mills theory in which the \mathbb{Z}_N 2-form flat gauge field (the 't Hooft flux) is explicitly treated as one of the dynamical variables. We observe that our HMC algorithm in the $SU(2)/\mathbb{Z}_2$ theory drastically reduces autocorrelation lengths of the topological charge and of a physical quantity which couples to slow modes in the conventional HMC simulation of the $SU(2)$ theory. Provided that sufficiently large lattice volumes are available, therefore, the HMC algorithm of the $SU(N)/\mathbb{Z}_N$ theory could be employed as an alternative for the simulation of the $SU(N)$ Yang–Mills theory, because local observables are expected to be insensitive to the difference between $SU(N)$ and $SU(N)/\mathbb{Z}_N$ in the large volume limit. A possible method to incorporate quarks [fermions in the fundamental representation of $SU(N)$ with the baryon number $1/N$] in this framework is also considered.
.....

Subject Index B01,B03,B31

1 Introduction

Recently, consideration on the Yang–Mills partition function with the 't Hooft flux [1] has revived [2–4], largely motivated by the perspective of the generalized symmetries [5], in particular in connection with the study in Ref. [6]. See also recent related studies [7–11], in which the 't Hooft flux plays the crucial role in analyses of the low-energy dynamics of gauge theory.

In the present paper, partially motivated by the above developments and partially motivated by the possibility of a geometrical definition of the fractional topological charge [12] in the $SU(N)$ Yang–Mills theory with the 't Hooft flux [13, 14], we carry out a hybrid Monte Carlo (HMC) lattice simulation of the $SU(2)/\mathbb{Z}_2$ Yang–Mills theory, in which the 't Hooft flux, the 2-form gauge field coupled to the \mathbb{Z}_2 1-form symmetry in the modern language, is dynamical. Traditionally, lattice simulations of the $SU(N)/\mathbb{Z}_N$ Yang–Mills theory are carried out by adopting the Wilson plaquette action in the adjoint representation, which is blind on the center \mathbb{Z}_N [15, 16]; in this way, nontrivial $SU(N)/\mathbb{Z}_N$ bundle structures are effectively summed over. See also Refs. [17, 18]. In this paper, instead, we treat the \mathbb{Z}_N 2-form flat gauge field explicitly as one of the dynamical variables; therefore, each gauge field configuration in the Monte Carlo simulation explicitly possesses the value of the \mathbb{Z}_N 2-form gauge field. In this sense, our idea is similar in spirit to the study in Ref. [19], in which the $SU(2)$ Yang–Mills partition function with a given fixed 't Hooft flux is computed, although we make the 't Hooft flux dynamical; see also Ref. [20] for an earlier Monte Carlo study with an explicit dynamical \mathbb{Z}_N 2-form gauge field. Here, we adopt (a variant of) the HMC simulation algorithm [21] having future applications of our method to lattice quantum chromodynamics (QCD) [$SU(3)$ Yang–Mills theory with fundamental quarks] in mind.

Meanwhile, for many years, it has been known that the conventional HMC algorithm on the periodic lattice suffers from the topological freezing problem, a phenomenon whereby the Monte Carlo update is stuck within a particular topological sector toward the continuum limit [22, 23]; see Ref. [24] and references therein for recent analyses. The HMC simulation with open boundary conditions [25], by activating in/out flows of topological charges from lattice boundaries, appears to remove topological barriers in between otherwise topological sectors and solve this problem. Here, we see an analogue with the HMC simulation in the $SU(N)/\mathbb{Z}_N$ gauge theory, in which the topological charge is shuffled by random dynamics of the \mathbb{Z}_N 2-form gauge field.

In continuum theory, the topological charge Q in the $SU(N)$ gauge theory on a 4-torus, T^4 , is defined by¹

$$Q := \int_{T^4} d^4x \frac{1}{32\pi^2} \varepsilon_{\mu\nu\rho\sigma} \text{tr} [F_{\mu\nu}(x) F_{\rho\sigma}(x)]. \quad (1.1)$$

In the $SU(N)$ Yang–Mills theory, $Q \in \mathbb{Z}$. However, in the $SU(N)/\mathbb{Z}_N$ theory, Q can be *fractional* as [13, 14]

$$Q = -\frac{1}{N} \frac{\varepsilon_{\mu\nu\rho\sigma} B_{\mu\nu} B_{\rho\sigma}}{8} + \mathbb{Z}, \quad (1.2)$$

where $B_{\mu\nu} \in \mathbb{Z}$ is the 't Hooft flux. Since $B_{\mu\nu}$ takes discrete values, we make a random choice of $B_{\mu\nu}$ in the HMC simulation of $SU(N)/\mathbb{Z}_N$ theory (see below). Then, this random choice inevitably shuffles the topological charge Q and we may expect that the topological sectors are efficiently sampled. We will observe that this expectation is actually true.

This paper is organized as follows. In Section 2, we briefly summarize basic facts about the $SU(N)/\mathbb{Z}_N$ theory, mainly to set up our lattice formulation on the periodic lattice of size L , $\Gamma := (\mathbb{Z}/L\mathbb{Z})^4$. Under a certain gauge fixing of the \mathbb{Z}_N 1-form gauge symmetry, the 2-form \mathbb{Z}_N gauge field takes a particular form (2.10) of the “ B -field” over which we carry out the “functional integral.” Section 3 is the main part of this paper. Since the B -field in Eq. (2.10) takes values in \mathbb{Z} and has no obvious conjugate momentum, we have to appropriately modify the HMC algorithm which is based on the molecular dynamics (MD) of continuous variables. In Section 3.1, we present our “halfway-updating” HMC algorithm which fulfills the detailed balance. The proof of the detailed balance is deferred to Appendix A. In Section 3.2, we study the autocorrelation function of the topological charge in the HMC history; we compare it in the $SU(2)$ theory (i.e., without the B -field) with the one in the $SU(2)/\mathbb{Z}_2$ theory (with the B -field). For the lattice topological charge, we employ the tree-level improved definition in Ref. [26], in which the lattice field smeared by the gradient flow [27] is substituted. We observe a drastic reduction of the autocorrelation in the HMC simulation in the latter theory as anticipated above. We also observe a similar reduction of the autocorrelation in the “energy-operator” $E(t)$ defined by the gradient flow [27]. As shown in Section 2, the difference between $SU(N)/\mathbb{Z}_N$ and $SU(N)$ can be understood as the difference in boundary conditions (and the sum over them) and thus local observables are expected to be insensitive to the difference between $SU(N)$ and $SU(N)/\mathbb{Z}_N$ in the large volume limit in these gapped theories. To have some idea on this point, we carry out an exploratory study on the finite size effect in the continuum extrapolation of the topological susceptibility. In Section 4, we present a possible method to incorporate fermions in the fundamental representation of $SU(N)$ (quarks) in this framework. This is achieved by gauging the baryon number $U(1)$,

¹ Throughout this paper, we take a convention that the field strength $F_{\mu\nu}(x)$ is a hermitian matrix.

$U(1)_B$, and embedding \mathbb{Z}_N into $SU(N) \times U(1)_B$. The $U(1)_B$ gauge boson unwanted for QCD is made super-heavy by the Stückelberg mechanism on lattice. Section 5 is devoted to a conclusion. In Appendix B, we present HMC histories and histograms of the topological charge for various lattice parameters.

2 $SU(N)/\mathbb{Z}_N$ Yang–Mills theory on T^4

The $SU(N)/\mathbb{Z}_N$ Yang–Mills theory on T^4 of size L in continuum can be defined as follows. See Refs. [3, 28]. We define boundary conditions of the $SU(N)$ gauge potential 1-form a on T^4 by

$$a(x + L\hat{\mu}) = g_\mu(x)^\dagger a(x) g_\mu(x) - i g_\mu(x)^\dagger d g_\mu(x), \quad (2.1)$$

where $x_\mu = 0$ and $\hat{\mu}$ is the unit vector in the μ direction; the transition functions $g_\mu(x)$ are $SU(N)$ -valued. Here, since the gauge potential behaves as the adjoint representation under the gauge transformation, one may relax the cocycle condition for the transition functions at $x_\mu = x_\nu = 0$ by \mathbb{Z}_N factors as

$$g_\mu(x) g_\nu(x + L\hat{\mu}) g_\mu(x + L\hat{\nu})^\dagger g_\nu(x)^\dagger = e^{2\pi i B_{\mu\nu}(x)/N} \mathbf{1}, \quad (2.2)$$

where $B_{\mu\nu}(x) \in \mathbb{Z}$ and $B_{\mu\nu}(x) = -B_{\nu\mu}(x)$. For the consistency of transition functions among “quadruple” overlaps, it is required that $B_{\mu\nu}(x)$ is flat modulo N , $dB = 0 \bmod N$. This defines the $SU(N)/\mathbb{Z}_N$ principal bundle and the $SU(N)/\mathbb{Z}_N$ Yang–Mills theory over T^4 . It can be shown that we may take constant $B_{\mu\nu}(x)$, $B_{\mu\nu}$. These integers are called the ’t Hooft fluxes.

It is well-understood how to implement this gauge theory on T^4 as a lattice gauge theory [29–31]; see also Appendix A.4 of Ref. [3] for a nice exposition. One first introduces link variables as $\tilde{U}(x, \mu) \sim \exp\left(i \int_x^{x+\hat{\mu}} a\right)$. Boundary conditions on T^4 are then defined by, as a

lattice counterpart of Eq. (2.1),²

$$\tilde{U}(x + L\hat{\mu}, \nu) = g_\mu(x)^\dagger \tilde{U}(x, \nu) g_\mu(x + \hat{\nu}), \quad (2.6)$$

where $x_\mu = 0$. We first regard link variables with $x_\rho = L$ for a certain ρ are all expressed by link variables with $x_\rho = 0$ by the boundary conditions (2.6). Then, we make the change of link variables from $\tilde{U} \rightarrow U$ by

$$\tilde{U}(x, \mu) = \begin{cases} U(x, \mu) g_\mu(x) & \text{for } x_\mu = L - 1, \\ U(x, \mu) & \text{otherwise.} \end{cases} \quad (2.7)$$

The new variables U are regarded as obeying periodic boundary conditions, $U(x + L\hat{\mu}, \nu) = U(x, \nu)$, where $x_\mu = 0$. Under this change of variables, one finds that the Boltzmann weight defined by the Wilson plaquette action acquires \mathbb{Z}_N factors as (letting β the lattice bare gauge coupling),

$$\begin{aligned} & \exp \left\{ \beta \sum_{x \in \Gamma} \sum_{\mu < \nu} \frac{1}{N} \text{Re tr} \left[\tilde{P}(x, \mu, \nu) - \mathbf{1} \right] \right\} \\ &= \exp \left\{ \beta \sum_{x \in \Gamma} \sum_{\mu < \nu} \frac{1}{N} \text{Re tr} \left[e^{-2\pi i B_{\mu\nu}(x)/N} P(x, \mu, \nu) - \mathbf{1} \right] \right\}, \end{aligned} \quad (2.8)$$

where plaquette variables are

$$\begin{aligned} \tilde{P}(x, \mu, \nu) &:= \tilde{U}(x, \mu) \tilde{U}(x + \hat{\mu}, \nu) \tilde{U}(x + \hat{\nu}, \mu)^\dagger \tilde{U}(x, \nu)^\dagger, \\ P(x, \mu, \nu) &:= U(x, \mu) U(x + \hat{\mu}, \nu) U(x + \hat{\nu}, \mu)^\dagger U(x, \nu)^\dagger, \end{aligned} \quad (2.9)$$

² Here is a side remark on the Wilson line wrapping around a cycle of T^4 : Under the ordinary 0-form gauge transformation,

$$\tilde{U}(x, \nu) \rightarrow \Omega(x)^\dagger \tilde{U}(x, \nu) \Omega(x + \hat{\nu}), \quad (2.3)$$

where $\Omega(x)$ is not necessarily periodic, the transition functions are transformed as

$$g_\mu(x) \rightarrow \Omega(x) g_\mu(x) \Omega(x + L\hat{\mu})^\dagger \quad (2.4)$$

and one sees that the cocycle condition (2.2) is invariant under this. The Wilson line of $\tilde{U}(x, \mu)$ thus should not contain the transition functions at the boundary, because under Eq. (2.3),

$$\begin{aligned} & \cdots \tilde{U}(x + (L-1)\hat{\mu}, \mu) \tilde{U}(x + L\hat{\mu}, \mu) \cdots \\ & \rightarrow \cdots \Omega(x + (L-1)\hat{\mu})^\dagger \tilde{U}(x + (L-1)\hat{\mu}, \mu) \tilde{U}(x + L\hat{\mu}, \mu) \Omega(x + (L+1)\hat{\mu}) \cdots \end{aligned} \quad (2.5)$$

and the integer field $B_{\mu\nu}(x)$ is given by the 't Hooft fluxes as

$$B_{\mu\nu}(x) = \begin{cases} B_{\mu\nu} & \text{for } x_\mu = L-1 \text{ and } x_\nu = L-1, \\ 0 & \text{otherwise.} \end{cases} \quad (2.10)$$

Note that this field is flat modulo N , $\partial_{[\rho} B_{\mu\nu]}(x) = 0 \bmod N$, where ∂_ρ denotes the lattice derivative. The particular form of $B_{\mu\nu}(x)$ in Eq. (2.10) is not unique and can be changed by the \mathbb{Z}_N 1-form gauge transformation, $U(x, \mu) \rightarrow e^{2\pi i z_\mu(x)/N} U(x, \mu)$, where $z_\mu(x) \in \mathbb{Z}$. The invariant characterization of $B_{\mu\nu}(x)$ is the total flux, $B_{\mu\nu} = \sum_{s,t=0}^{L-1} B_{\mu\nu}(x + s\hat{\mu} + t\hat{\nu}) \bmod N$. In what follows, we call the \mathbb{Z}_N 2-form gauge field and/or the 't Hooft flux simply, “ B -field” in a moderate abuse of language.

In the next section, we carry out an HMC simulation of the system defined by the second line of Eq. (2.8), employing configurations of the B -field of the particular form shown in Eq. (2.10). This implies that we work in a particular gauge of the \mathbb{Z}_N 1-form gauge symmetry; the observables thus should be invariant under the \mathbb{Z}_N 1-form gauge transformation, $U(x, \mu) \rightarrow e^{2\pi i z_\mu(x)/N} U(x, \mu)$ and $B_{\mu\nu}(x) \rightarrow B_{\mu\nu}(x) + \partial_\mu z_\nu(x) - \partial_\nu z_\mu(x) \bmod N$.

3 Numerical experiments

3.1 “Halfway-updating” HMC algorithm

In our study, we basically follow the HMC algorithm [21],³ having possible future applications to lattice QCD in mind (see Section 4). However, since the B -field takes values in \mathbb{Z} and has no obvious conjugate momentum, we have to appropriately modify the HMC algorithm. We see that the following “halfway-updating” HMC algorithm fulfills the detailed balance, a sufficient condition for the Markov chain Monte Carlo to reproduce the equilibrium distribution with a given Boltzmann weight.

Let U and B be the initial configuration of the gauge field and the B -field, respectively. Then,

- (1) Generate the initial momentum π being conjugate to U by the Gaussian distribution $P_G(\pi) \sim e^{-\pi^2/2}$.
- (2) Via the leapfrog method, evolve π and U with respect to the Hamiltonian $H(U, \pi, B) := (1/2)\pi^2 + S(U, B)$, where the action $S(U, B)$ is given by the exponent of the second line of Eq. (2.8), by the MD time $\tau/2$. This gives the mapping $\{U, \pi\} \xrightarrow{\tau/2} \{\check{U}, \check{\pi}\}$.

³ Our numerical codes can be found in <https://github.com/o-morikawa/Gaugefields.jl>, which is based on `Gaugefields.jl` in the JuliaQCD package [32].

- (3) Update the B -field as $B \rightarrow B'$ in a probability $P_F(B \rightarrow B')$. We assume that $P_F(B \rightarrow B') = P_F(B' \rightarrow B)$ for any pair (B, B') . In our actual simulations, we set $B'_{\mu\nu}$ for each pair (μ, ν) by a uniform random number in $\{0, 1, \dots, N-1\}$.⁴
- (4) Again evolve fields as $\{\check{U}, \check{\pi}\} \xrightarrow{\tau/2} \{U', \pi'\}$ by the MD but now with respect to the Hamiltonian $H(\check{U}, \check{\pi}, B') := (1/2)\check{\pi}^2 + S(\check{U}, B')$ by the MD time $\tau/2$.
- (5) Accept the new configuration $\{U', \pi', B'\}$ under the probability (the Metropolis test)

$$P_A(\{U, \pi, B\} \rightarrow \{U', \pi', B'\}) = \min \left[1, e^{-\Delta H} \right], \quad (3.1)$$

where $\Delta H := H(U', \pi', B') - H(U, \pi, B)$.

- (6) Go back to the first step.

As shown in Appendix A, this algorithm fulfills the detailed balance.

The lattice parameters we used are summarized in Tables 1 and 2. In our HMC simulation for the $SU(2)/\mathbb{Z}_2$ theory, for all lattice parameters, the length of one HMC step τ (“one trajectory”) is 1.0 in lattice units ($\Delta\tau = 0.02$ times 25 MD steps for the “half-way” and in total there are 50 MD steps for one HMC step). For our largest and finest lattice ($\beta = 2.6$ and $L = 20$), the Metropolis acceptance was $\sim 86\%$. We also carry out the HMC simulation for the $SU(2)$ theory using the conventional HMC algorithm. For this also, for all lattice parameters, $\tau = 1.0$ in lattice units ($\Delta\tau = 0.02$ and there are 50 MD steps).

For the $SU(2)$ theory (i.e., without the B -field), we referred to the mapping between β and $a\sqrt{\sigma}$, where σ is the string tension, given in Ref. [34]. We used this mapping also for the $SU(2)/\mathbb{Z}_2$ theory (i.e., with the B -field). This point might be subtle, however, because the conventional Wilson line operator is not gauge invariant in the $SU(2)/\mathbb{Z}_2$ theory. A more satisfactory way would be to use the gradient flow [27] such that the value of a/\sqrt{t} , where t/a^2 is the flow time in lattice units, at which the expectation value of the local operator (3.2) $t^2\langle E(t) \rangle$ becomes (say) 0.3. In any case, in the $SU(2)/\mathbb{Z}_2$ theory, the dependence of the

⁴ A technical note on this prescription: Given a \mathbb{Z}_N 2-cochain field $Z_{\mu\nu}(x)$ on T^4 being flat in the sense that $\prod_c Z_{\mu\nu}(x) = 1$, where the oriented product \prod_c is taken on 6 faces of a 3D cube c , one can associate the flux in Eq. (2.10) with $0 \leq B_{\mu\nu} < N$ in the following way. First, define $\check{B}_{\mu\nu}(x)$ by $Z_{\mu\nu}(x) = e^{-2\pi i \check{B}_{\mu\nu}(x)/N}$ and $0 \leq \check{B}_{\mu\nu}(x) < N$. This $\check{B}_{\mu\nu}(x)$ is flat but generally only modulo N , i.e., $\partial_{[\rho} \check{B}_{\mu\nu]}(x) = 0 \bmod N$. On T^4 , one can construct a \mathbb{Z} 2-cocycle $M_{\mu\nu}(x)$ such that $\bar{B}_{\mu\nu}(x) := \check{B}_{\mu\nu}(x) - NM_{\mu\nu}(x)$ satisfies $\partial_{[\rho} \bar{B}_{\mu\nu]}(x) = 0$ ($\bar{B}_{\mu\nu}(x)$ provides the integral lift of $H^2(T^4, \mathbb{Z}_N)$ to $H^2(T^4, \mathbb{Z})$). An explicit method to construct $M_{\mu\nu}(x)$ on a periodic hypercubic lattice is given in Section 4.2 of Ref. [33]. This $\bar{B}_{\mu\nu}(x)$ is 1-form gauge equivalent to $B_{\mu\nu}(x)$ of the form in Eq. (2.10). Finally, after the local shift by multiples of N , $B_{\mu\nu}(x) \rightarrow B_{\mu\nu}(x) + NN_{\mu\nu}(x)$, where $N_{\mu\nu}(x) \in \mathbb{Z}$, one can restrict the range of $B_{\mu\nu}$ in Eq. (2.10) into $0 \leq B_{\mu\nu} < N$. This argument shows that if the action and observables are invariant under the 1-form gauge transformation and the local shift of $B_{\mu\nu}(x)$ by multiples of N , then our algorithm amounts to generating the \mathbb{Z}_N 2-cochain field $Z_{\mu\nu}(x)$ on T^4 .

Table 1: The lattice parameters in our HMC simulation in the $SU(2)/\mathbb{Z}_2$ theory.

β	L	$a\sqrt{\sigma}$	$La\sqrt{\sigma}$	N configs.
2.4	8	0.2673	2.138	5000
2.5	12	0.186	2.23	5000
2.6	16	0.1326	2.122	1744
2.4	10	0.2673	2.673	5000
2.5	14	0.186	2.60	5387
2.6	20	0.1326	2.652	1046

Table 2: The lattice parameters in our HMC simulation in the $SU(2)$ theory.

β	L	$a\sqrt{\sigma}$	$La\sqrt{\sigma}$	N configs.
2.4	8	0.2673	2.138	5000
2.5	12	0.186	2.23	5000
2.6	16	0.1326	2.122	1635

integrated autocorrelation time on the lattice spacing is quite weak and this subtlety should not crucially change our conclusion.

For each of lattice parameters, we stored configurations per each 10 units of MD time (i.e., per every 10 trajectories).

3.2 Autocorrelation functions

We are primarily interested in the HMC history of the topological charge Q . It is possible to construct a geometrical definition of the lattice topological charge Q in the $SU(N)$ theory with the B -field, which exactly ensures fractional values (1.2), by combining the seminal idea in Ref. [35] and the \mathbb{Z}_N 1-form gauge invariance [12]. Its actual implementation, however, appears quite complicated. Here, therefore, we instead employ the following definition of Q on the basis of the gradient flow [27].

We adopt the tree-level improved linear combination of the clover and rectangular definitions given in Ref. [26], by including the B -field in each of the plaquettes for the 1-form gauge invariance. We substitute a field configuration smeared by the gradient flow in this definition. Here, the gradient flow refers to the lattice action in the second line of Eq. (2.8) and thus the

flow equation itself depends also on the B -field.⁵ Therefore, the gradient flow acts so that the modified plaquette variables $e^{2\pi i B_{\mu\nu}} P(x, \mu, \nu)$, *not* $P(x, \mu, \nu)$, become smooth.⁶ Since the B -field is not differentiable (it takes values in \mathbb{Z}), this difference in the meaning of the smoothness has a drastic effect which can make the topological charge fractional.⁷ In the present exploratory study, we measure the topological charge of flowed configurations only at a flow time $t = (0.7L)^2/8$ in lattice units, where L is the lattice size, corresponding to the smeared or diffused length $\sim \sqrt{8t} = 0.7L$; in this paper, we do not study how the results depend on this choice of the flow time.

In Fig. 1, we depict the HMC history of the topological charge Q in the $SU(2)/\mathbb{Z}_2$ theory ($\beta = 2.6$ and $L = 16$). We clearly observe that Q takes (approximately) fractional values as expected in the present $SU(2)/\mathbb{Z}_2$ case, $Q = 1/2 + \mathbb{Z}$. Also, the distribution of Q spreads in a wide range without any obvious autocorrelation in the HMC history; it appears that the topological sectors are shuffled by the dynamical effect of the B -field.

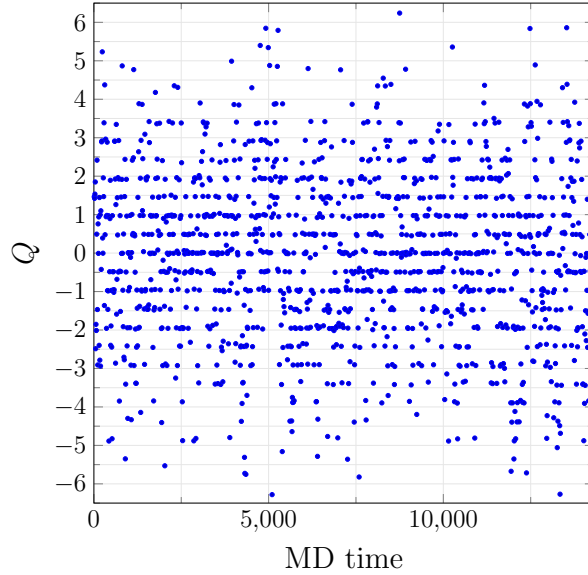


Fig. 1: The HMC history of the topological charge Q in the $SU(2)/\mathbb{Z}_2$ theory. $\beta = 2.6$ and $L = 16$.

⁵ We do not consider the “flow” of the B -field itself. We admit that the renormalizability [36, 37] of this gradient flow with a fixed B -field is an open problem, although we expect it because the local dynamics should be insensitive to whether we simulate $SU(N)$ or $SU(N)/\mathbb{Z}_N$.

⁶ In other words, the smoothness on the lattice, the admissibility [35, 38], is replaced by $\|\mathbf{1} - e^{2\pi i B_{\mu\nu}} P(x, \mu, \nu)\| < \varepsilon$ for a certain small constant ε [12].

⁷ We would like to thank Yuya Tanizaki for originally sharing this idea with us.

For a comparison, in Fig. 2, we depict the HMC history of the topological charge Q in the HMC simulation of the $SU(2)$ theory. In contrast, we clearly observe the tendency that Q is stuck and the topological freezing of $O(500)$ MD time.

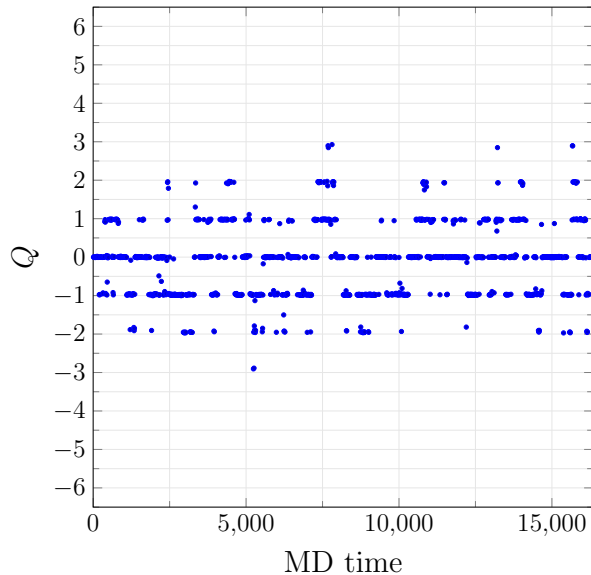


Fig. 2: The HMC history of the topological charge Q in the $SU(2)$ theory (i.e., without the B -field). $\beta = 2.6$ and $L = 16$. The topological freezing is clearly seen.

The HMC history of Q for other lattice parameters in conjunction with the histogram of Q are presented in Appendix B.

We expect that the autocorrelation length increases as the system approaches the critical point (i.e., the continuum limit). In Fig. 3, we plot the normalized autocorrelation functions of the topological charge Q in the $SU(2)$ theory as a function of the MD time; we follow the definition of the autocorrelation function in Appendix E of Ref. [39].

Figure 3 is for the $SU(2)$ theory without the B -field. In Fig. 4, we plot the normalized autocorrelation function of Q in the $SU(2)/\mathbb{Z}_2$ theory with the dynamical B -field. We observe that the autocorrelation is drastically reduced. Figure 5 shows the normalized autocorrelation function of the topological charge for the latter three rows of Table 1.

In Fig. 6, we plot the integrated autocorrelation lengths (we follow the definition in Appendix E of Ref. [39]) of the topological charge Q and its square Q^2 as a function of the lattice spacing a in units of the string tension σ . The general consideration [25] indicates that the integrated autocorrelation length in the HMC algorithm increases as a^{-2} . We fairly well observe this scaling behavior in Fig. 6. However, the slope is quite small for the $SU(2)/\mathbb{Z}_2$ theory with our HMC algorithm.

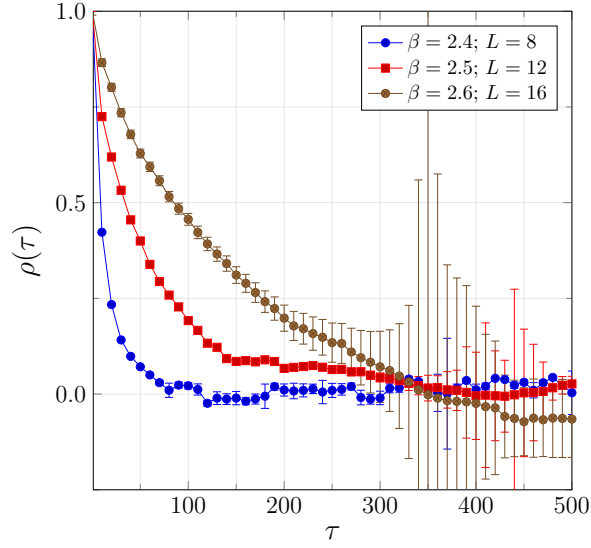


Fig. 3: The normalized autocorrelation functions of the topological charge Q in the conventional HMC simulation of the $SU(2)$ theory. The horizontal axis is the MD time. The cases in Table 2 with approximately identical physical lattice sizes are plotted.

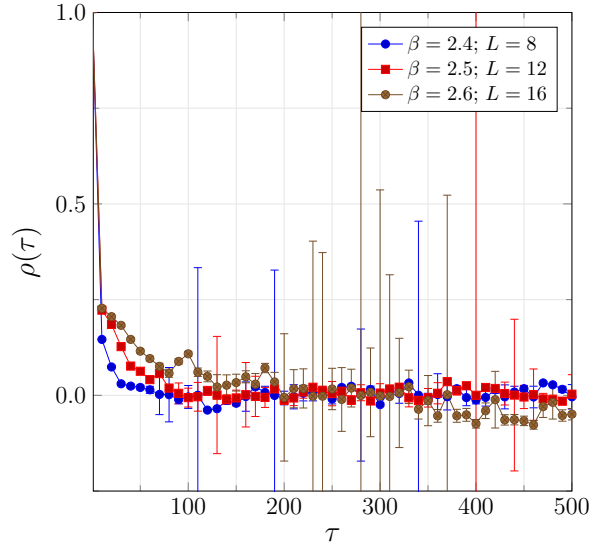


Fig. 4: The normalized autocorrelation functions of the topological charge Q in the HMC simulation of the $SU(2)/\mathbb{Z}_2$ theory (i.e., with the B -field). The horizontal axis is the MD time. The cases of first three rows in Table 1 with approximately identical physical lattice sizes are plotted. The lattice parameters are identical to those in Fig. 3.

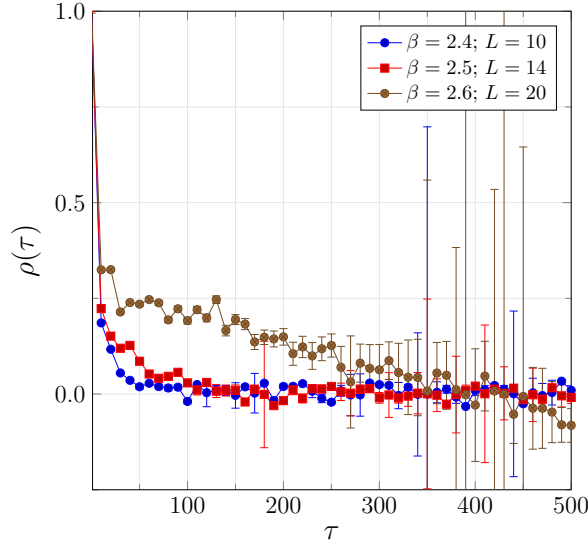


Fig. 5: The normalized autocorrelation functions of the topological charge Q in the HMC simulation of the $SU(2)/\mathbb{Z}_2$ theory. The horizontal axis is the MD time. The cases of latter three rows of Table 1 of approximately identical physical lattice sizes are plotted.

The drastic reduction of the autocorrelation in Q and in Q^2 is, although quite impressive, somehow expected because the random choice of the B -field inevitably shuffles the topological charge. This does not, however, necessarily imply that the autocorrelation of any observables is reduced in the $SU(2)/\mathbb{Z}_2$ theory. To examine this point, we measure the HMC history of another observable which is expected to have a large overlap with slow modes of the HMC algorithm. It is given by the so-called “energy-operator” [25] (we implicitly assume the average over $x \in \Gamma$),

$$E(t) := \frac{1}{2} \text{tr} [F_{\mu\nu}(t, x) F_{\mu\nu}(t, x)], \quad (3.2)$$

where the field strength on the right-hand side is given by the gradient flow at the flow time t [27] (in the $SU(2)/\mathbb{Z}_2$ theory, we multiply each of plaquettes by the B -field). The flow time is fixed to $t = (0.7L)^2/8$. In Figs. 7 and 8, we plot the HMC histories of $E(t)$ for the $SU(2)$ theory and for the $SU(2)/\mathbb{Z}_2$ theory, respectively ($\beta = 2.6$ and $L = 16$). In Fig. 7, we clearly observe the large autocorrelation of $O(100)$ MD time, whereas in the $SU(2)/\mathbb{Z}_2$ theory of Fig. 8, we do not see any notable autocorrelation; in fact, the integrated autocorrelation time is of $O(20)$ MD time in the latter. These observations strongly indicate that our HMC algorithm for the $SU(2)/\mathbb{Z}_2$ or more generally the $SU(N)/\mathbb{Z}_N$ theory reduces the autocorrelation in general physical quantities drastically.

Finally, to have some idea how large is the finite size effect which provides the difference between $SU(2)/\mathbb{Z}_2$ and $SU(2)$ on local observables, in Figs. 9 and 10, we plot the topological

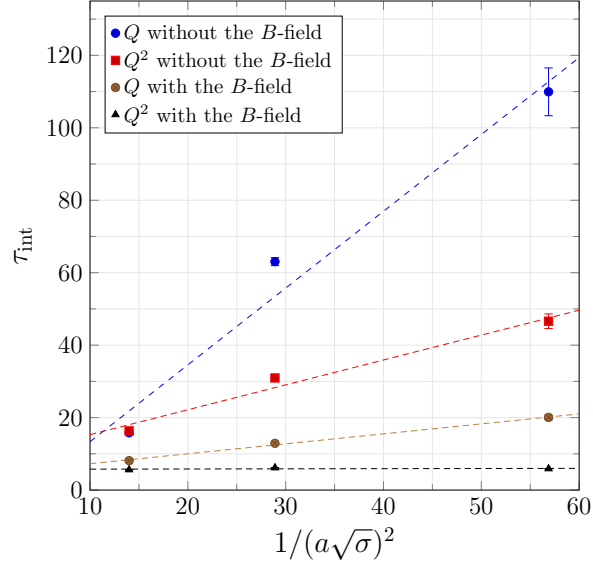


Fig. 6: The integrated autocorrelation lengths in lattice units of the topological charge Q and of the square Q^2 as the function of the lattice spacing. For the cases in the first three rows of Table 1 and Table 2.

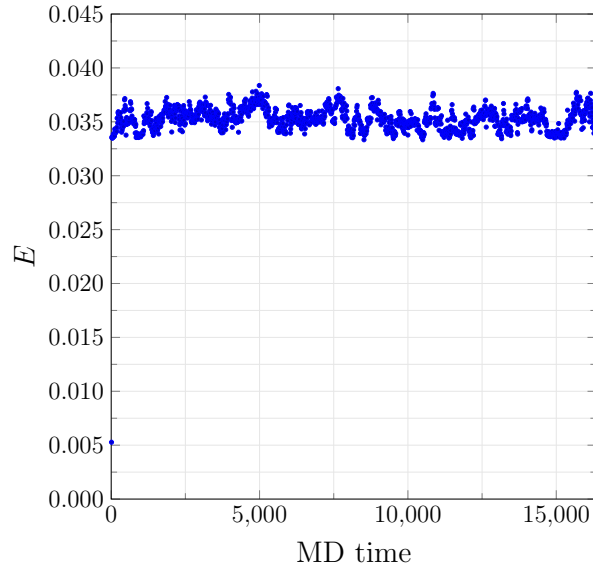


Fig. 7: The HMC history of $E(t)$ (3.2) in the $SU(2)$ theory (i.e., without the B -field). $\beta = 2.6$ and $L = 16$.

susceptibility

$$\chi_t := \frac{1}{(La)^4} \langle Q^2 \rangle \quad (3.3)$$

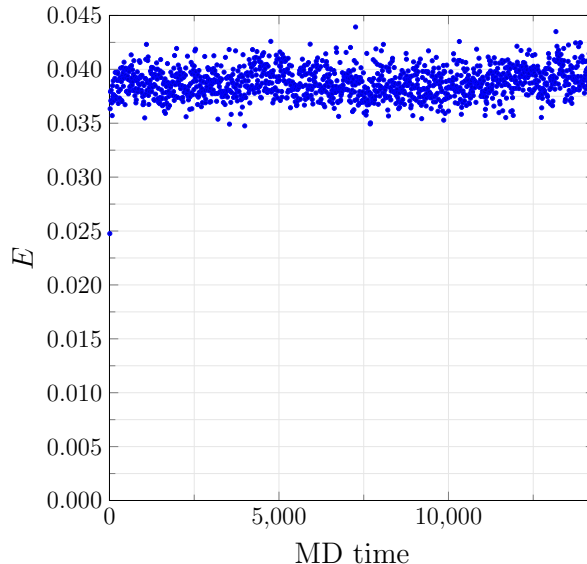


Fig. 8: The HMC history of $E(t)$ (3.2) in the $SU(2)/\mathbb{Z}_2$ theory (i.e., with the B -field). $\beta = 2.6$ and $L = 16$.

in units of the string tension σ . For all lattice parameters, the first 50 configurations (500 MD time) are omitted for thermalization and statistical errors are estimated by the jackknife method with a bin size 40, corresponding to 40 configurations and 400 units of MD time. Although the error bars for the $SU(2)/\mathbb{Z}_2$ and $SU(2)$ theories in Figs. 9 and 10 are of almost the same order, we observed that the jackknife errors in the $SU(2)/\mathbb{Z}_2$ cases are much more quickly saturated compared to the $SU(2)$ cases, as expected from the shortness of the autocorrelation.

In Fig. 11, we combined the two continuum extrapolations in Fig. 9 as a function of the physical lattice size. A naive linear extrapolation of central values to the infinite volume appears consistent with the result in the $SU(2)$ theory [34], considering large statistical error bars in our results. To conclude the validity of the present approach to the $SU(2)$ theory from the $SU(2)/\mathbb{Z}_2$ theory, however, we need further statistics for larger and finer lattices.

4 Incorporation of fundamental quarks

One clearly wants to incorporate matter fields in the present framework. The incorporation of the adjoint matter fields such as the gaugino in the $\mathcal{N} = 1$ supersymmetric Yang–Mills theory would be straightforward at least in principle because it is blind to the center part of the gauge group $SU(N)$, \mathbb{Z}_N ; thus $SU(N)/\mathbb{Z}_N$ can be gauged. A better control on errors in the topological susceptibility could be quite useful for finding a supersymmetric point of

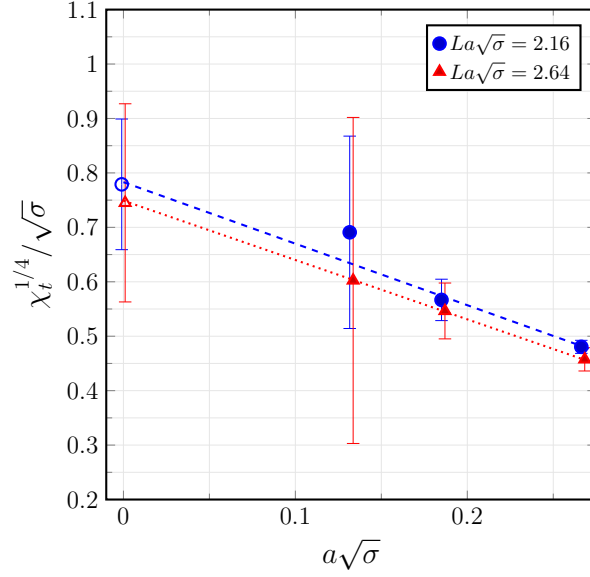


Fig. 9: The continuum extrapolations of the topological susceptibility χ_t (3.3) in the $SU(2)/\mathbb{Z}_2$ theory. The two lines correspond to two sequences corresponding to two different physical volumes; the first/blue line corresponds to the first three lattice parameters in Table 1 whereas the second/red line corresponds to the latter three lattice parameters in Table 1.

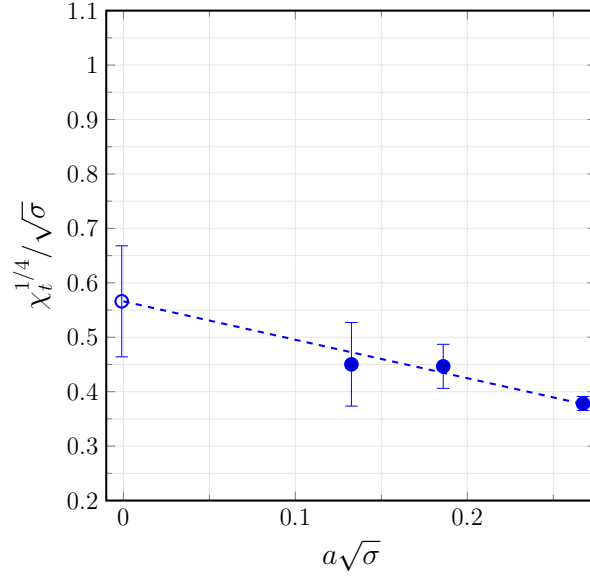


Fig. 10: The continuum extrapolation of the topological susceptibility χ_t (3.3) in the $SU(2)$ theory. The result is consistent with the one in Ref. [34], $\chi_t^{1/4}/\sqrt{\sigma} = 0.486(10)$.

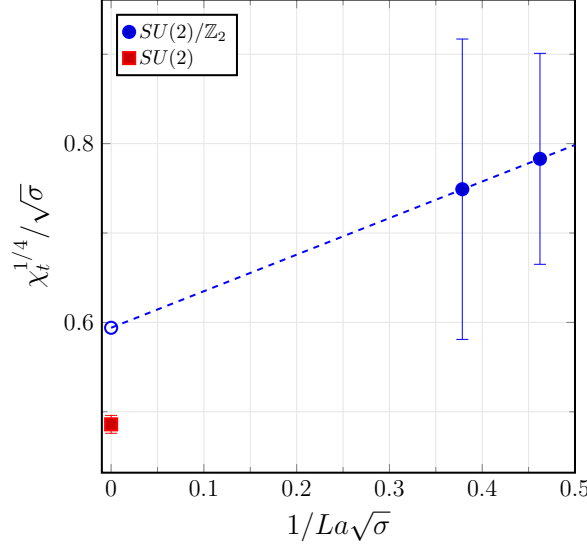


Fig. 11: Continuum extrapolations in Fig. 9 as a function of the physical volume. A naive linear extrapolation of central values to the infinite volume appears consistent with the result in the $SU(2)$ theory, indicated by $SU(2)$ in the figure, $\chi_t^{1/4}/\sqrt{\sigma} = 0.486(10)$ [34], considering large statistical error bars in our results.

the bare lattice gluino mass parameter [40], since a massless fermion implies the vanishing of the topological susceptibility.

It is, however, not obvious whether it is possible to incorporate “quarks,” fermions in the fundamental representation of $SU(N)$ and this point can be an obstacle to extending the present framework to lattice QCD. In what follows, we consider a possible method to avoid this obstruction.

First, when the B -field is fixed, i.e., when it is *not dynamical*, one may incorporate quarks as follows [3]: We first define boundary conditions of the fundamental fermions by

$$\begin{aligned}\tilde{\psi}(x + L\hat{\mu}) &= e^{-i\alpha_\mu(x)/N} g_\mu(x)^\dagger \tilde{\psi}(x), \\ \tilde{\bar{\psi}}(x + L\hat{\mu}) &= \tilde{\bar{\psi}}(x) g_\mu(x) e^{i\alpha_\mu(x)/N},\end{aligned}\tag{4.1}$$

where $x_\mu = 0$. Here, transition functions $g_\mu(x)$ are identified with those in Eq. (2.1) and $e^{-i\alpha_\mu(x)/N}$ is the transition functions of the baryon number $U(1)$ ($U(1)_B$) principal bundle; the factor $1/N$ arises since we set the quark $U(1)_B$ charge $1/N$. Then, postulating the cocycle condition at $x_\mu = x_\nu = 0$,

$$e^{i\alpha_\mu(x)/N} e^{i\alpha_\nu(x+L\hat{\mu})/N} e^{-i\alpha_\mu(x+L\hat{\nu})/N} e^{-i\alpha_\nu(x)/N} = e^{-2\pi i B_{\mu\nu}/N},\tag{4.2}$$

the \mathbb{Z}_N factors in this relation cancel the \mathbb{Z}_N factors in Eq. (2.2); the fermion fields can thus be consistently defined on T^4 although it belongs to the fundamental representation

of $SU(N)$ [3]. Corresponding to Eq. (4.1), the $U(1)_B$ gauge potential 1-form A_B in the charge $1/N$ representation possess the boundary conditions

$$A_B(x + L\hat{\mu}) = A_B(x) + \frac{1}{N}d\alpha_\mu(x), \quad (4.3)$$

where $x_\mu = 0$. This $U(1)_B$ bundle is characterized by the first Chern numbers,

$$\int_{\mu\nu \text{ plane}} dA_B = 2\pi \left(\frac{B_{\mu\nu}}{N} + \mathbb{Z} \right), \quad (4.4)$$

where we have used Eqs. (4.3) and (4.2). Note that we can introduce mass terms for quarks in this setup as far as they preserve the $U(1)_B$ symmetry, not necessarily the flavor $SU(N_f)$ [3]. Thus, this system is quite different from the \mathbb{Z}_N QCD [41, 42] with the $SU(N)$ flavor symmetry.

In lattice gauge theory, we introduce the $U(1)_B$ link variables as $\tilde{U}_B(x, \mu) \sim \exp\left(i \int_x^{x+\hat{\mu}} A_B\right)$. Corresponding to Eq. (4.3), $\tilde{U}_B(x, \mu)$ obey boundary conditions

$$\tilde{U}_B(x + L\hat{\mu}, \nu) = e^{-i\alpha_\mu(x)/N} \tilde{U}_B(x, \nu) e^{i\alpha_\mu(x+\hat{\nu})/N}. \quad (4.5)$$

Under the change of link variables analogous to Eq. (2.7),

$$\tilde{U}_B(x, \mu) = \begin{cases} U_B(x, \mu) e^{i\alpha_\mu(x)/N} & \text{for } x_\mu = L - 1, \\ U_B(x, \mu) & \text{otherwise,} \end{cases} \quad (4.6)$$

we find that

$$\tilde{P}_B(x, \mu, \mu) = e^{2\pi i B_{\mu\nu}(x)/N} P_B(x, \mu, \nu), \quad (4.7)$$

where

$$\begin{aligned} \tilde{P}_B(x, \mu, \nu) &:= \tilde{U}_B(x, \mu) \tilde{U}_B(x + \hat{\mu}, \nu) \tilde{U}_B(x + \hat{\nu}, \mu)^* \tilde{U}_B(x, \nu)^*, \\ P_B(x, \mu, \nu) &:= U_B(x, \mu) U_B(x + \hat{\mu}, \nu) U_B(x + \hat{\nu}, \mu)^* U_B(x, \nu)^*, \end{aligned} \quad (4.8)$$

and $B_{\mu\nu}(x)$ is given by Eq. (2.10). The variables U_B are regarded as obeying periodic boundary conditions, $U_B(x + L\hat{\mu}, \nu) = U_B(x, \nu)$, where $x_\mu = 0$. Using the boundary conditions, Eqs. (4.1), (4.5) and (2.3), and then the change of variables, Eqs. (2.7) and (4.6), we find that lattice hopping terms of the fundamental fermion take the following forms,

$$\begin{aligned} \tilde{\bar{\psi}}(x) \tilde{U}_B(x, \mu) \tilde{U}(x, \mu) \tilde{\psi}(x + \hat{\mu}) &= \bar{\psi}(x) U_B(x, \mu) U(x, \mu) \psi(x + \hat{\mu}), \\ \tilde{\bar{\psi}}(x) \tilde{U}(x - \hat{\mu}, \mu)^\dagger \tilde{U}_B(x - \hat{\mu}, \mu)^* \tilde{\psi}(x - \hat{\mu}) &= \bar{\psi}(x) U(x - \hat{\mu}, \mu)^\dagger U_B(x - \hat{\mu}, \mu)^* \psi(x - \hat{\mu}), \end{aligned} \quad (4.9)$$

everywhere on the lattice Γ including boundaries. In this expression, fermion variables $\psi(x)$ and $\bar{\psi}(x)$ are understood to obey the periodic boundary conditions, $\psi(x + L\hat{\mu}) = \psi(x)$ and $\bar{\psi}(x + L\hat{\mu}) = \bar{\psi}(x)$ for $x_\mu = 0$.

So far, the $U(1)_B$ gauge field $\tilde{U}_B(x, \mu)$ is regarded as a non-dynamical background. However, since the B -field is dynamical in the $SU(N)/\mathbb{Z}_N$ theory and $\tilde{U}_B(x, \mu)$ depends on the B -field through the boundary conditions (4.5), $\tilde{U}_B(x, \mu)$ inevitably becomes dynamical in the $SU(N)/\mathbb{Z}_N$ theory.

The Wilson plaquette action for the $U(1)_B$ gauge field would be

$$\begin{aligned} & \exp \left\{ \beta_B \sum_{x \in \Gamma} \sum_{\mu < \nu} \text{Re} \left[\tilde{P}_B(x, \mu, \nu) - 1 \right] \right\} \\ &= \exp \left\{ \beta_B \sum_{x \in \Gamma} \sum_{\mu < \nu} \text{Re} \left[e^{2\pi i B_{\mu\nu}(x)/N} P_B(x, \mu, \nu) - 1 \right] \right\}, \end{aligned} \quad (4.10)$$

where β_B is the bare coupling. However, of course, the dynamical $U(1)_B$ gauge field is unwanted for the sake to simulate QCD. For a possible solution on this point, we make the $U(1)_B$ gauge boson super-heavy by the Stückelberg mechanism on the lattice. That is, we introduce a $U(1)$ -valued dynamical scalar field $\Omega(x) \in U(1)$ and add the lattice action

$$\begin{aligned} S_{\text{Stückelberg}} &:= \frac{1}{2} \sum_{x \in \Gamma} \sum_{\mu} \left[1 - \tilde{\Omega}(x + \hat{\mu})^* \tilde{U}_B(x, \mu)^N \tilde{\Omega}(x) \right] \left[\tilde{\Omega}(x)^* \tilde{U}_B(x, \mu)^N \tilde{\Omega}(x + \hat{\mu}) - 1 \right] \\ &= \frac{1}{2} \sum_{x \in \Gamma} \sum_{\mu} \left[1 - \Omega(x + \hat{\mu})^* U_B(x, \mu)^N \Omega(x) \right] \left[\Omega(x)^* U_B(x, \mu)^N \Omega(x + \hat{\mu}) - 1 \right]. \end{aligned} \quad (4.11)$$

In this expression, $\tilde{\Omega}(x)$ obeys the twisted boundary conditions, $\tilde{\Omega}(x + L\hat{\mu}) = e^{-i\alpha_\mu(x)} \tilde{\Omega}(x)$ ($x_\mu = 0$), while $\Omega(x)$ obeys the periodic boundary conditions, $\Omega(x + L\hat{\mu}) = \Omega(x)$. $S_{\text{Stückelberg}}$ is invariant under the $U(1)_B$ 0-form and \mathbb{Z}_N 1-form gauge transformations. The gauge fixing of $U(1)_B$ of the form $\Omega(x) = 1$ then shows that the $U(1)_B$ gauge boson acquires the mass of $O(a^{-2})$ and we expect that this freedom decouples in the continuum limit.

5 Conclusion

In this paper, we carried out an HMC simulation of the $SU(2)/\mathbb{Z}_2$ Yang–Mills theory, in which the \mathbb{Z}_N 2-form flat gauge field (the 't Hooft flux) is treated as a dynamical variable. We observed that our HMC algorithm in the $SU(2)/\mathbb{Z}_2$ theory drastically reduces the auto-correlation lengths of the topological charge and of the “energy-operator” defined by the

gradient flow. We thus infer that, provided that sufficiently large lattice volumes are available, the HMC simulation of the $SU(N)/\mathbb{Z}_N$ theory could be employed as an alternative for the simulation of the $SU(N)$ Yang–Mills theory with a very efficient sampling of topological sectors. Toward applications in lattice QCD, we also presented a possible method to incorporate quarks. Further tests on these ideas are to be awaited.

Acknowledgments

We would like to thank Yui Hayashi, Yuki Nagai, Yuya Tanizaki, Akio Tomiya, and Hiromasa Watanabe for helpful discussions. We appreciate the opportunity of the discussion during the YITP–RIKEN iTHEMS conference “Generalized symmetries in QFT 2024” (YITP-W-24-15) in execution of this work. Numerical computations in this paper were carried out on Genkai, a supercomputer system of the Research Institute for Information Technology (RIIT), Kyushu University. The work of M.A. was supported by Kyushu University Innovator Fellowship Program in Quantum Science Area. O.M. acknowledges the RIKEN Special Postdoctoral Researcher Program. The work of H.S. was partially supported by Japan Society for the Promotion of Science (JSPS) Grant-in-Aid for Scientific Research, JP23K03418.

A Halfway HMC fulfills the detailed balance

In this appendix, we give a proof that the halfway HMC algorithm in Section 3.1 fulfills the detailed balance, a sufficient condition for the Markov chain Monte Carlo to reproduce the equilibrium distribution.

Since B and B' are fixed within the MD time from 0 to $\tau/2$ and from $\tau/2$ to τ , respectively, the leapfrog integrator possesses the invertibility, i.e., if there exists an MD trajectory such that $\{U, \pi\}_B \xrightarrow{\tau/2} \{\check{U}, \check{\pi}\}_B$, then $\{\check{U}, -\check{\pi}\}_B \xrightarrow{\tau/2} \{U, -\pi\}_B$ holds (if there exists an MD trajectory such that $\{\check{U}, \check{\pi}\}_{B'} \xrightarrow{\tau/2} \{U', \pi'\}_{B'}$, then $\{U', -\pi'\}_{B'} \xrightarrow{\tau/2} \{\check{U}, -\check{\pi}\}_{B'}$ holds). That is, probabilities associated with the MD satisfy

$$\begin{aligned} P_M(\{U, \pi\} \xrightarrow{\tau/2} \{\check{U}, \check{\pi}\})|_B &= P_M(\{\check{U}, -\check{\pi}\} \xrightarrow{\tau/2} \{U, -\pi\})|_B, \\ P_M(\{\check{U}, \check{\pi}\} \xrightarrow{\tau/2} \{U', \pi'\})|_{B'} &= P_M(\{U', -\pi'\} \xrightarrow{\tau/2} \{\check{U}, -\check{\pi}\})|_{B'}, \end{aligned} \quad (\text{A1})$$

We also know that the Metropolis test probability in Eq. (3.1) satisfies

$$e^{-H(U, \pi, B)} P_A(\{U, \pi, B\} \rightarrow \{U', \pi', B'\}) = e^{-H(U', \pi', B')} P_A(\{U', \pi', B'\} \rightarrow \{U, \pi, B\}). \quad (\text{A2})$$

We note that the total probability of the present halfway HMC is given by

$$\begin{aligned}
& P(\{U, B\} \rightarrow \{U', B'\}) \\
&= \int d\pi d\pi' P_G(\pi) P_M(\{U, \pi\} \xrightarrow{\tau/2} \{\check{U}, \check{\pi}\})|_B P_F(B \rightarrow B') P_M(\{\check{U}, \check{\pi}\} \xrightarrow{\tau/2} \{U', \pi'\})|_{B'} \\
&\quad \times P_A(\{U, \pi, B\} \rightarrow \{U', \pi', B'\}).
\end{aligned} \tag{A3}$$

From this, noting $H(U, \pi, B) = (1/2)\pi^2 + S(U, B)$ and Eq. (A2), we find

$$\begin{aligned}
& e^{-S(U, B)} P(\{U, B\} \rightarrow \{U', B'\}) \\
&= \int d\pi d\pi' e^{-H(U', \pi', B')} \\
&\quad \times P_M(\{U, \pi\} \xrightarrow{\tau/2} \{\check{U}, \check{\pi}\})|_B P_F(B \rightarrow B') P_M(\{\check{U}, \check{\pi}\} \xrightarrow{\tau/2} \{U', \pi'\})|_{B'} \\
&\quad \times P_A(\{U', \pi', B'\} \rightarrow \{U, \pi, B\}).
\end{aligned} \tag{A4}$$

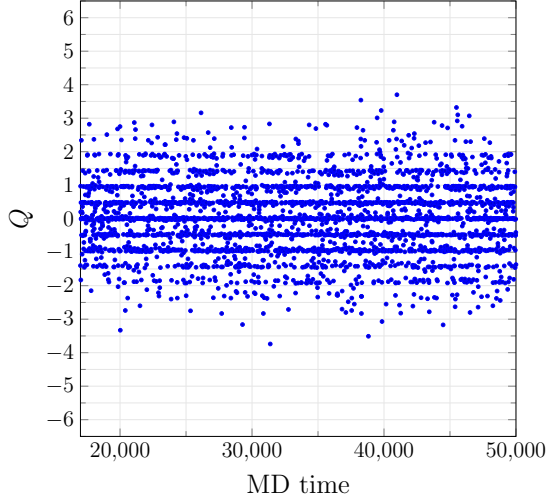
Then, noting $H(U', \pi', B') = (1/2)\pi'^2 + S(U', B')$ and Eq. (A1),

$$\begin{aligned}
& e^{-S(U, B)} P(\{U, B\} \rightarrow \{U', B'\}) \\
&= e^{-S(U', B')} \int d\pi d\pi' P_G(\pi') \\
&\quad \times P_M(\{U', -\pi'\} \xrightarrow{\tau/2} \{\check{U}, -\check{\pi}\})|_{B'} P_F(B' \rightarrow B) P_M(\{\check{U}, -\check{\pi}\} \xrightarrow{\tau/2} \{U, -\pi\})|_B \\
&\quad \times P_A(\{U', \pi', B'\} \rightarrow \{U, \pi, B\}) \\
&= e^{-S(U', B')} P(\{U', B'\} \rightarrow \{U, B\}),
\end{aligned} \tag{A5}$$

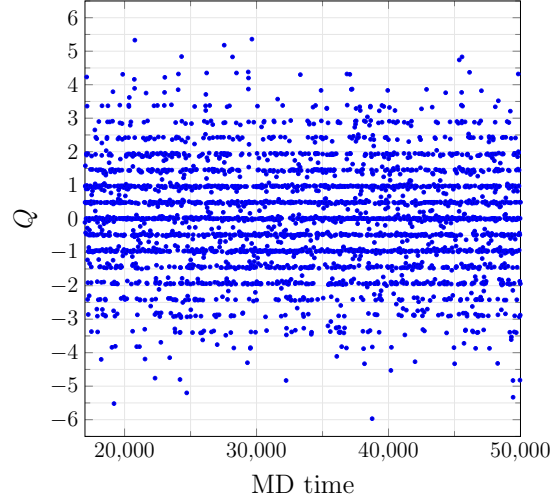
where we have used $P_F(B \rightarrow B') = P_F(B' \rightarrow B)$. This is the detailed balance.

B The HMC history and the histogram of Q .

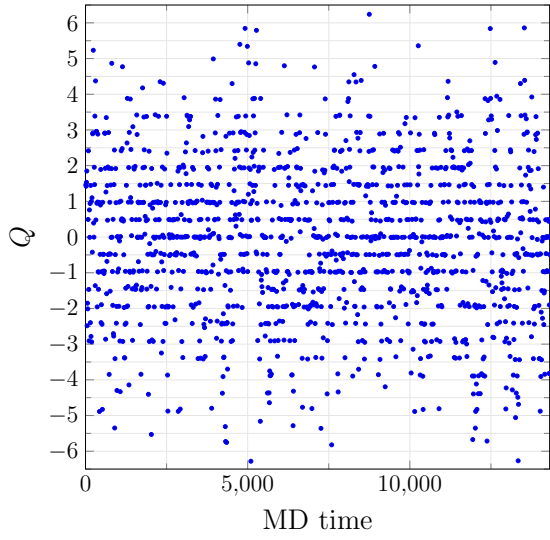
In this appendix, we present HMC histories and histograms of the topological charge Q in the $SU(2)/\mathbb{Z}_2$ and $SU(2)$ theories in Figs. B1 and B2, respectively.



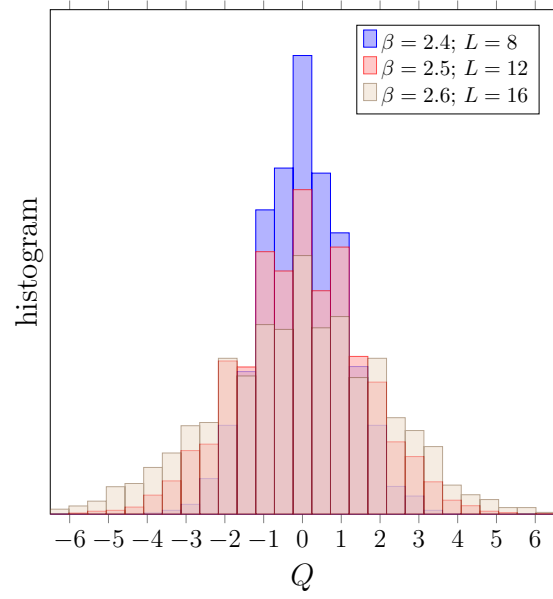
(a) $\beta = 2.4$ and $L = 8$.



(b) $\beta = 2.5$ and $L = 12$.

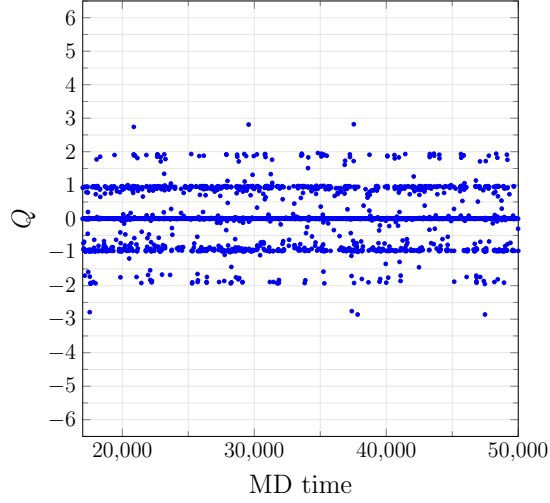


(c) $\beta = 2.6$ and $L = 16$.

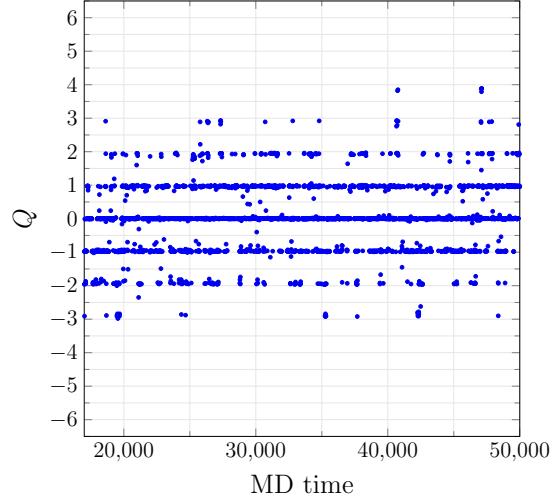


(d) The histogram of Q .

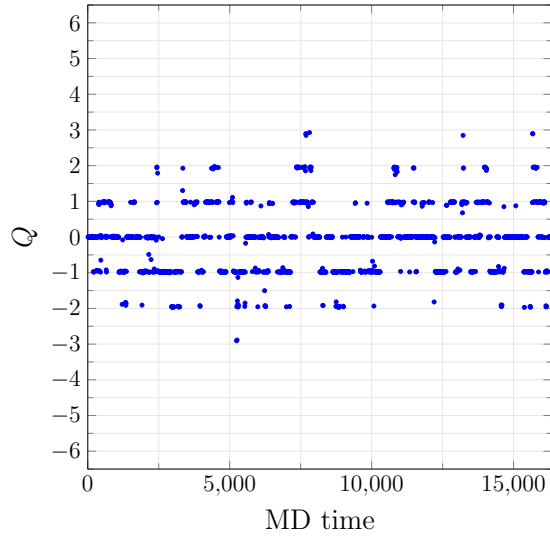
Fig. B1: The HMC histories and the histogram of Q , for the $SU(2)/\mathbb{Z}_2$ theory (i.e., with the B -field).



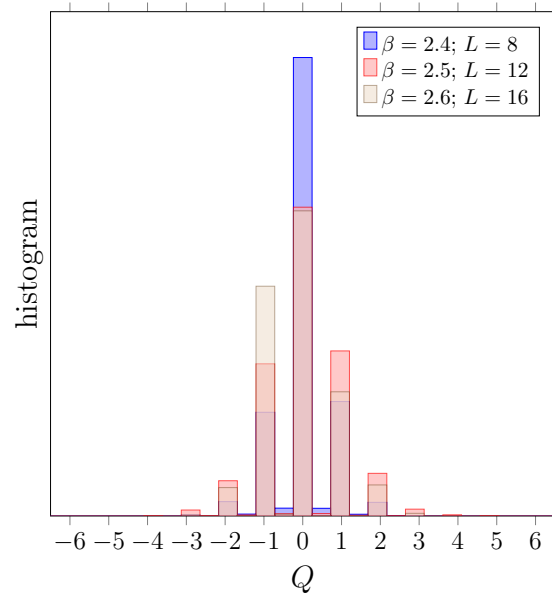
(a) $\beta = 2.4$ and $L = 8$.



(b) $\beta = 2.5$ and $L = 12$.



(c) $\beta = 2.6$ and $L = 16$.



(d) The histogram of Q .

Fig. B2: The HMC histories and the histogram of Q , for the $SU(2)$ theory (i.e., without the B -field).

References

- [1] G. 't Hooft, Nucl. Phys. B **153**, 141-160 (1979) doi:10.1016/0550-3213(79)90595-9
- [2] R. Kitano, T. Suyama and N. Yamada, JHEP **09**, 137 (2017) doi:10.1007/JHEP09(2017)137 [arXiv:1709.04225 [hep-th]].
- [3] Y. Tanizaki and M. Ünsal, PTEP **2022**, no.4, 04A108 (2022) doi:10.1093/ptep/ptac042 [arXiv:2201.06166 [hep-th]].
- [4] M. Nguyen, Y. Tanizaki and M. Ünsal, JHEP **08**, 013 (2023) doi:10.1007/JHEP08(2023)013 [arXiv:2306.02485 [hep-th]].
- [5] D. Gaiotto, A. Kapustin, N. Seiberg and B. Willett, JHEP **02**, 172 (2015) doi:10.1007/JHEP02(2015)172 [arXiv:1412.5148 [hep-th]].
- [6] D. Gaiotto, A. Kapustin, Z. Komargodski and N. Seiberg, JHEP **05**, 091 (2017) doi:10.1007/JHEP05(2017)091 [arXiv:1703.00501 [hep-th]].
- [7] M. Yamazaki and K. Yonekura, JHEP **07**, 088 (2017) doi:10.1007/JHEP07(2017)088 [arXiv:1704.05852 [hep-th]].
- [8] Y. Hayashi, Y. Tanizaki and H. Watanabe, JHEP **10**, 146 (2023) doi:10.1007/JHEP10(2023)146 [arXiv:2307.13954 [hep-th]].
- [9] Y. Hayashi and Y. Tanizaki, JHEP **08**, 001 (2024) doi:10.1007/JHEP08(2024)001 [arXiv:2402.04320 [hep-th]].
- [10] Y. Hayashi and Y. Tanizaki, Phys. Rev. Lett. **133**, no.17, 171902 (2024) doi:10.1103/PhysRevLett.133.171902 [arXiv:2405.12402 [hep-th]].
- [11] Y. Hayashi, T. Misumi and Y. Tanizaki, JHEP **05**, 194 (2025) doi:10.1007/JHEP05(2025)194 [arXiv:2410.21392 [hep-th]].
- [12] M. Abe, O. Morikawa, S. Onoda, H. Suzuki and Y. Tanizaki, JHEP **08**, 118 (2023) doi:10.1007/JHEP08(2023)118 [arXiv:2303.10977 [hep-lat]].
- [13] G. 't Hooft, Commun. Math. Phys. **81**, 267-275 (1981) doi:10.1007/BF01208900
- [14] P. van Baal, Commun. Math. Phys. **85**, 529 (1982) doi:10.1007/BF01403503
- [15] I. G. Halliday and A. Schwimmer, Phys. Lett. B **101**, 327 (1981) doi:10.1016/0370-2693(81)90055-1
- [16] M. Creutz and K. J. M. Moriarty, Nucl. Phys. B **210**, 50-58 (1982) doi:10.1016/0550-3213(82)90248-6
- [17] R. G. Edwards, U. M. Heller and R. Narayanan, Phys. Lett. B **438**, 96-98 (1998) doi:10.1016/S0370-2693(98)00951-4 [arXiv:hep-lat/9806011 [hep-lat]].
- [18] P. de Forcrand and O. Jahn, Nucl. Phys. B **651**, 125-142 (2003) doi:10.1016/S0550-3213(02)01123-9 [arXiv:hep-lat/0211004 [hep-lat]].
- [19] T. G. Kovács and E. T. Tomboulis, Phys. Rev. Lett. **85**, 704-707 (2000) doi:10.1103/PhysRevLett.85.704 [arXiv:hep-lat/0002004 [hep-lat]].
- [20] I. G. Halliday and A. Schwimmer, Phys. Lett. B **102**, 337-340 (1981) doi:10.1016/0370-2693(81)90630-4
- [21] S. Duane, A. D. Kennedy, B. J. Pendleton and D. Roweth, Phys. Lett. B **195**, 216-222 (1987) doi:10.1016/0370-2693(87)91197-X
- [22] L. Del Debbio, H. Panagopoulos and E. Vicari, JHEP **08**, 044 (2002) doi:10.1088/1126-6708/2002/08/044 [arXiv:hep-th/0204125 [hep-th]].
- [23] S. Schaefer *et al.* [ALPHA], Nucl. Phys. B **845**, 93-119 (2011) doi:10.1016/j.nuclphysb.2010.11.020 [arXiv:1009.5228 [hep-lat]].
- [24] C. Bonanno, G. Clemente, M. D'Elia, L. Maio and L. Parente, JHEP **08**, 236 (2024) doi:10.1007/JHEP08(2024)236 [arXiv:2404.14151 [hep-lat]].
- [25] M. Lüscher and S. Schaefer, JHEP **07**, 036 (2011) doi:10.1007/JHEP07(2011)036 [arXiv:1105.4749 [hep-lat]].
- [26] C. Alexandrou, A. Athenodorou and K. Jansen, Phys. Rev. D **92**, no.12, 125014 (2015) doi:10.1103/PhysRevD.92.125014 [arXiv:1509.04259 [hep-lat]].
- [27] M. Lüscher, JHEP **08**, 071 (2010) [erratum: JHEP **03**, 092 (2014)] doi:10.1007/JHEP08(2010)071 [arXiv:1006.4518 [hep-lat]].
- [28] A. Kapustin and N. Seiberg, JHEP **04**, 001 (2014) doi:10.1007/JHEP04(2014)001 [arXiv:1401.0740 [hep-th]].
- [29] G. Mack and V. B. Petkova, Annals Phys. **125**, 117 (1980) doi:10.1016/0003-4916(80)90121-9
- [30] A. Ukawa, P. Windey and A. H. Guth, Phys. Rev. D **21**, 1013 (1980) doi:10.1103/PhysRevD.21.1013
- [31] E. Seiler, Lect. Notes Phys. **159**, 1-192 (1982)
- [32] Y. Nagai and A. Tomiya, “JuliaQCD: Portable lattice QCD package in Julia language,” [arXiv:2409.03030 [hep-lat]].
- [33] M. Abe, O. Morikawa and H. Suzuki, PTEP **2023**, no.2, 023B03 (2023) doi:10.1093/ptep/ptad009 [arXiv:2210.12967 [hep-th]].
- [34] M. J. Teper, [arXiv:hep-th/9812187 [hep-th]].
- [35] M. Lüscher, Commun. Math. Phys. **85**, 39 (1982) doi:10.1007/BF02029132

- [36] M. Lüscher and P. Weisz, JHEP **02**, 051 (2011) doi:10.1007/JHEP02(2011)051 [arXiv:1101.0963 [hep-th]].
- [37] K. Hieda, H. Makino and H. Suzuki, Nucl. Phys. B **918**, 23-51 (2017) doi:10.1016/j.nuclphysb.2017.02.017 [arXiv:1604.06200 [hep-lat]].
- [38] P. Hernández, K. Jansen and M. Lüscher, Nucl. Phys. B **552**, 363-378 (1999) doi:10.1016/S0550-3213(99)00213-8 [arXiv:hep-lat/9808010 [hep-lat]].
- [39] M. Lüscher, Comput. Phys. Commun. **165**, 199-220 (2005) doi:10.1016/j.cpc.2004.10.004 [arXiv:hep-lat/0409106 [hep-lat]].
- [40] G. Curci and G. Veneziano, Nucl. Phys. B **292**, 555-572 (1987) doi:10.1016/0550-3213(87)90660-2
- [41] H. Kouno, Y. Sakai, T. Makiyama, K. Tokunaga, T. Sasaki and M. Yahiro, J. Phys. G **39**, 085010 (2012) doi:10.1088/0954-3899/39/8/085010
- [42] T. Iritani, E. Itou and T. Misumi, JHEP **11**, 159 (2015) doi:10.1007/JHEP11(2015)159 [arXiv:1508.07132 [hep-lat]].